

Point and interval evaluation of nanoparticles censored sample in the spray process

Hanieh Panahi^{1,*}, Saeid Asadi²

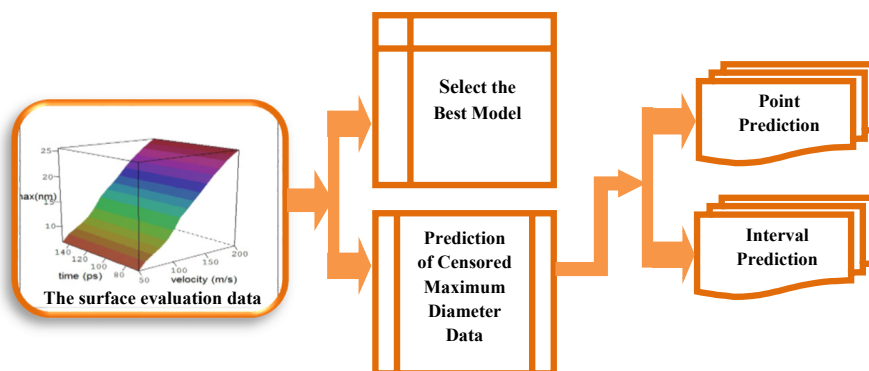
¹ Department of Mathematics and Statistics, Lahijan branch, Islamic Azad University, Lahijan, Iran

² Department of Mechanical Engineering, Payame Noor University (PNU), Tehran, Iran

HIGHLIGHTS

- Evaluation of the maximum spreading diameter of nanoparticle data on hydrophobic surface was studied.
- The generalized inverted exponential model was proposed as an appropriate model.
- The Markov Chain Monte Carlo procedure and likelihood approach were used to predict the censored data.

GRAPHICAL ABSTRACT



ARTICLE INFO

Article history:

Received 20 January 2019

Revised 6 October 2019

Accepted 6 November 2019

Keywords:

Censored data

Classical and Bayesian prediction

Generalized inverted exponential model

Maximum diameter

Nanoparticle

ABSTRACT

A good nano coating depends on the quality of the collision and spreading behavior of the nanoparticles. Unfortunately, in many cases, nanoparticle spreading data has not been recorded. In this paper, we have extended the evaluation model to predict the unavailable or censored maximum spreading diameter of nanoparticle data. Different point and interval methods have been considered for this problem. Choosing Bayesian evaluation, the Markov Chain Monte Carlo (MCMC) has been proposed as an efficient procedure for estimating the predictive inference for future observation. An important implication of the present study is that the censored maximum diameter data can be predicted well using the proposed methods. Results showed the proposed point predictions are close to real data, the predictive intervals contain the real values, and it verifies the applicability of the prediction techniques for real problems.

* Corresponding author: Tel.: +9813-33229081 ; Fax: +9813-33228701 ; E-mail address: panahi@liau.ac.ir

DOI: 10.22104/JPST.2019.3437.1143

1. Introduction

Coating by nanoparticle spreading performs a critical role in numerous novel industrial processes such as plasma spray coating, nano self-assembling, nano safeguard coatings, and ink-jet printing. Currently, the observations on some experimental units, even in well-planned experiments on industrial processes, are sometimes not available. Missing and unavailable data in nano-coating research is a common problem. Maximum diameter of a nanoparticle, one of the most important parameters during particle spreading on a surface, may be unavailable at times. In the coating process, liquid particles spread on the surface until they reach a maximum diameter where the liquid surface tension and viscosity overcame inertial forces, after which droplet recoil off the surface. Although the maximum diameter is an important parameter, only a few studies on this topic are found in the literature. For example, Maroo and Chung simulated the impact of an argon nanodroplet on a homogeneous platinum wall using molecular dynamics [1]. They evaluated interface markers, interfacial fit, and contact angles and observed the Leidenfrost effect for a wall temperature of 300 K for both cases of surface wettability. Sedighi *et al.* analyzed the process of a single nanodroplet impact onto a surface with molecular dynamics simulation (MD) [2]. They observed that the dynamic contact angle, spreading diameter, and advancing and receding periods exhibit a strong dependence on droplet size. Asadi proposed a novel computational fluid dynamics and molecular kinetic theory (CFD-MK) method to simulate nanodroplet impact onto a solid surface [3]. He evaluated the spreading behavior for wettable, partially wettable, and non-wettable surfaces. Hai-Bao *et al.* studied the dynamic processes of a nanodroplet impacting on hydrophobic surfaces at a nano dimension level [4]. They simulated the dynamic process of nanodroplet impact on hydrophobic surfaces with different wetting properties and showed the variations of diameter on surfaces with contact angles of 110° and 130° under different velocities. Li *et al.* examined the impact of a nanodroplet on a flat solid surface using molecular dynamics simulations [5]. They compared the obtained maximum spreading factors with previous models in the literature and reduced the mean relative error in predicting the maximum spreading factor for cases of nanodroplet impact. Using molecular

dynamics simulations, Kobayashi *et al.* investigated nanodroplet spreading at the early stage after the impact by changing the magnitude of the intermolecular force between the liquid and wall molecules [6]. They found that as the intermolecular force between the liquid and wall becomes stronger, the normalized spreading diameter of the first molecular layer on the wall remains less dependent on the impact velocity. Asadi simulated the impact of nanodroplets on an oblique surface using molecular dynamics and showed that nanodroplet spread increased only slightly by increasing the collision angle but increased hugely with increasing velocity [7]. Panahi and Asadi studied the distribution of nano and micro droplets spreading when droplets impacted an oblique surface [8]. They indicated that generalized exponential distribution shows better results than the other distributions for nano- and microdroplets spreading data.

We observed that experiments and dynamic simulations for obtaining data are expensive and time-consuming. A literature survey also indicated a lack of published information on the prediction of maximum diameter spreading of nanodroplets in coating processes. So, the main aim of this paper is to focus on the estimation and prediction of an unavailable (censored) maximum diameter sample belonging to a future sample based on the currently available sample, which is known as the informative sample. Many authors have considered predictive inference to solve challenging issues in engineering, chemistry, business, and biomedical sciences. Khan *et al.* proposed predictive inference on the basis of a doubly censored sample from a Rayleigh model [9]. Ahmed considered the Bayesian estimation and prediction of censored data [10]. Panahi and Asadi studied the modeling problem using splashing data and then predicted the censored data [11]. Chiang *et al.* introduced different model selection approaches for estimating and predicting the censored sample [12]. Basak and Balakrishnan considered the problem of predicting unit survival times from exponential distribution, which are not reported in a simple step-stress testing experiment [13].

In this paper, we first verified whether a generalized inverted exponential model can be used to fit this dataset, and then identify the related different point and interval prediction methods. For comparison purposes, we computed the prediction estimates and prediction intervals needed for future observation. The maximum

likelihood and Bayesian approaches were chosen to be studied as the point prediction methods. Also, the pivotal quantity and Bayesian viewpoint were proposed for constructing the prediction intervals. A schematic workflow representing the steps of this work is summarized in Fig. 1.

2. Model Description

2.1. Probability density function (pdf)

The generalized inverted exponential distribution was introduced in the literature by Abouammoh and Alshingiti as a generalization of the inverted exponential distribution [14]. This distribution can be used for many applications, including accelerated life testing, coating processes, sea currents, wind speeds, etc. [15-17]. Let T be a positive random variable of maximum diameter spreading of nanodroplets with the probability density function $f_r(t)$ and the cumulative distribution function $F_r(t)$ as:

$$f_r(t) = f(t; \alpha, \beta) = \frac{\alpha\beta}{t^2} \exp(-\beta/t) [1 - \exp(-\beta/t)]^{\alpha-1} \quad (1)$$

$$t > 0, \alpha > 0, \beta > 0$$

$$F_r(t) = F(t, \alpha, \beta) = 1 - [1 - \exp(-\beta/t)]^\alpha \quad (2)$$

$$t > 0, \alpha > 0, \beta > 0$$

where, α and β are the shape and scale parameters, respectively. This model (generalized inverted exponential model) has a unimodal and right skewed density function, depending on the shape parameter. In Fig. 2, we have plotted the probability density function

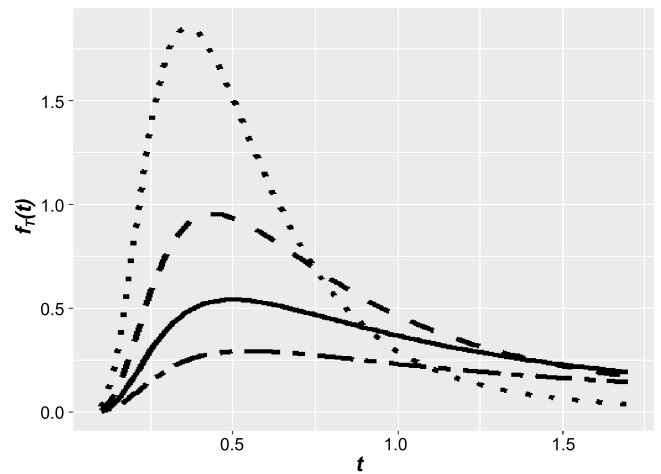


Fig. 2. The pdfs of model 1 for $\beta = 1$ and $\alpha = 0.5$ (dash-dotted line), $\alpha = 1$ (solid line), $\alpha = 2$ (dashed line), and $\alpha = 5$ (dotted line).

of the generalized inverted exponential model for some parameters.

Some known models are found to be sub-models of the proposed model. For instance,

- If $\alpha=1$ then Eq. (1) reduces to the inverted exponential model.
- If the random variable T has a generalized inverted exponential model, then the random variable $\tilde{T} = \frac{1}{T}$, has the generalized exponential model.

2.2. The hazard and reliability functions

The hazard function is the ratio of the probability density function to the reliability function. It is a reliability measure that play a crucial role in real data analysis. The hazard function analysis is used in many fields such as epidemiology, manufacturing, medicine, actuarial statistics, reliability engineering, and economics. The hazard function is a metric which

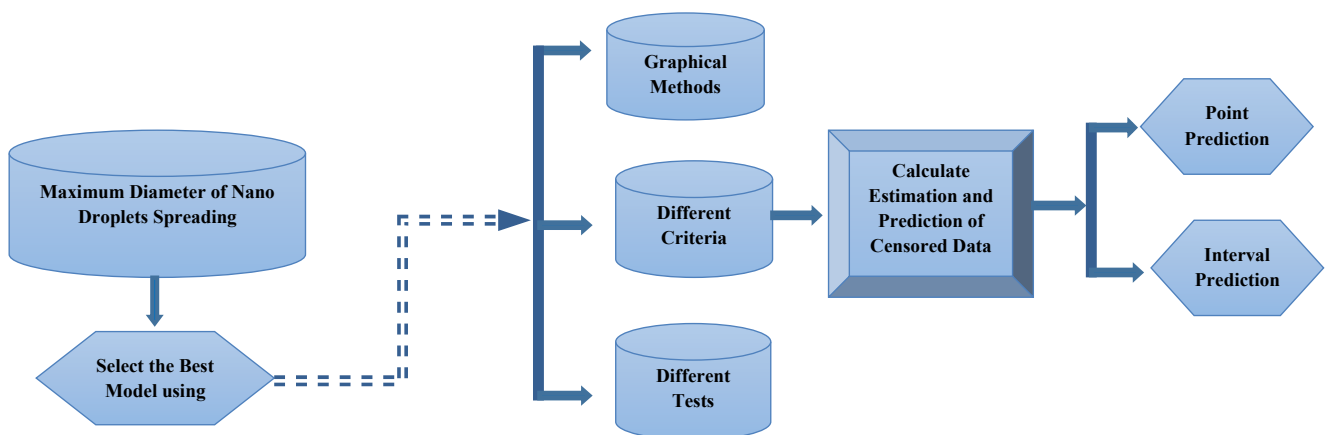


Fig. 1. The flow chart of the major contribution of this study.

is usually used to identify the appropriate probability distribution of a particular mechanism. Based on $f_r(t)$ and $F_r(t)$, the reliability and hazard functions of T are given by Eqs. (3) and (4), respectively [18].

$$r_T(t) = 1 - F_T(t) = [1 - \exp(-\beta/t)]^\alpha \quad (3)$$

$$t > 0, \alpha > 0, \beta > 0$$

$$h_T(t) = \frac{f_T(t)}{1 - F_T(t)} = \frac{\alpha\beta}{t^2} \exp(-\beta/t)(1 - \exp(-\beta/t))^{-1} \quad (4)$$

In Fig. 3, we have plotted the hazard and reliability functions for $\beta = 1$ and different choices of α ($\alpha = 0.5, 1, 2, 5$). Fig. 3(a) shows that the curve increases at the initial stage but starts to decrease at some points; this indicates that the proposed model could be unimodal. These figures indicate that model 1 shows good statistical behavior. Also, Fig. 3(b) indicates that the reliability function for all values of decreases with time.

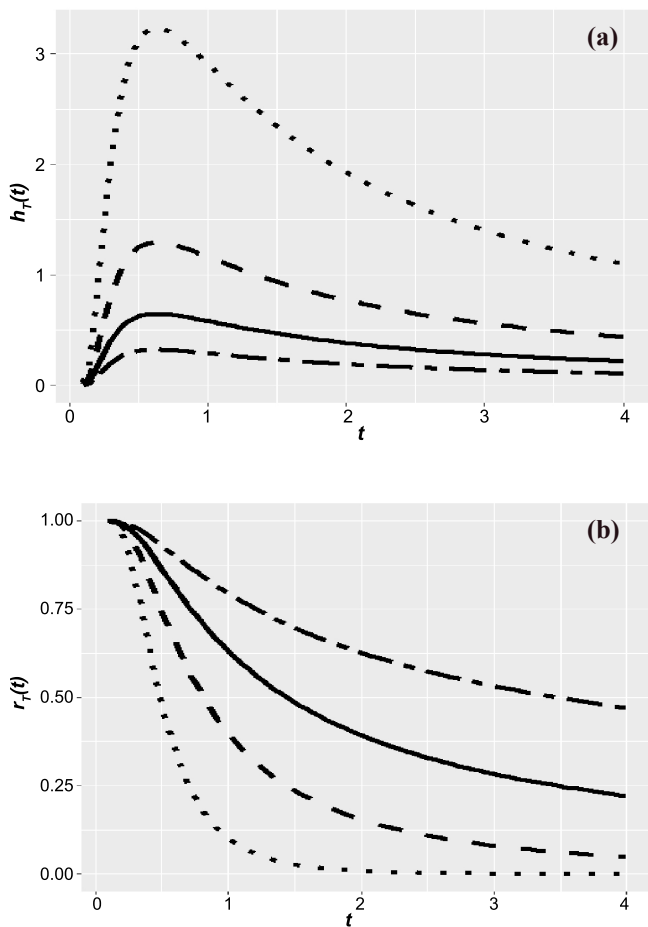


Fig. 3. The hazard (a) and reliability (b) functions of model 1 for $\beta = 1$ and $\alpha = 0.5$ (dash-dotted line), $\alpha = 1$ (solid line), $\alpha = 2$ (dashed line), and $\alpha = 5$ (dotted line).

2.3. Quantile Function and Median

The Quantile function is given by Eq. (5).

$$Q(u) = F^{-1}(u) \quad (5)$$

Where u is a random variable uniformly distributed on $(0,1)$ and $F(u)$ is a cumulative distribution function. Therefore, the corresponding quantile function for model 1 can be written as:

$$Q(u) = \frac{-\beta}{\ln(1 - (1-u)^{1/\alpha})} \quad (6)$$

We obtain the median by substituting $u = 0.5$, in Eq. (6). So, we have:

$$Median(T) = \frac{-\beta}{\ln(1 - (1-0.5)^{1/\alpha})} \quad (7)$$

Also, model 1 can be simulated using the following transformation:

$$T = \frac{-\beta}{\ln(1 - (1-U)^{1/\alpha})} \quad (8)$$

3. Point and Interval prediction of Censored data

In this section, we consider different evaluations of the censored data. Let T_1, \dots, T_n be the sample from the maximum diameter spreading of nanodroplets. Experiments and mechanical simulation are time-consuming. So, we considered the data as a censored sample and predicted the unobserved (censored) data. For this purpose, we supposed that $T_{1:n}, \dots, T_{D:n}$ is the observed data and we cannot observe the $T_{D+1:n}, \dots, T_{n:n}$. The main aim is to obtain the prediction of $\mathfrak{S} = T_{s+d:n}$ ($s = 1, 2, \dots, n-D$) of all the $n-D$ censored units based on observed data $T_{1:n}, \dots, T_{D:n}$. We supposed two times (T_1^* and T_2^*) and observed three different cases for the observed data. Thus, based on Eq. (1) and using the left truncated model at T^* , the joint density function of the censored (generalized Type-II hybrid censored) sample is as follows [19]:

$$f(t) = \frac{n!}{(n-D)!} \prod_{i=1}^D \frac{\alpha\beta}{t_i^2} \exp(-\beta/t_i) [1 - \exp(-\beta/t_i)]^{\alpha-1} (1 - \exp(-\beta/T^*))^\alpha \quad (9)$$

where, $D = \{D_1, r \text{ or } D_2\}$ and $T^* = \{T_1^*, T_{r:n} \text{ or } T_2^*\}$ (for more details about this censoring scheme see [19,20]).

3.1. Point Prediction

In this subsection, we obtain several point predictions for $\mathfrak{Z} = T_{s+D:n}$ ($s = 1, 2, \dots, n-D$) based on $T_{1:n}, \dots, T_{D:n}$ using likelihood and the Bayesian approach.

3.1.1. Likelihood prediction approach

We considered the prediction of $\mathfrak{Z} = T_{s+D:n}$ based on $T_{1:n}, \dots, T_{D:n}$ using a likelihood approach (PLP). Based on Eq. (1), the conditional density of $\mathfrak{Z} = T_{s+D:n}$ ($s = 1, 2, \dots, n-D$) is given by [21,22]:

$$f(\mathfrak{Z}|T) = s \binom{n-D}{s} \frac{\alpha\beta}{\mathfrak{Z}^2} \exp(-\beta/\mathfrak{Z}) [1 - \exp(-\beta/\mathfrak{Z})]^{\alpha-1} \left[(1 - \exp(-\beta/T^*))^\alpha - (1 - \exp(-\beta/\mathfrak{Z}))^\alpha \right]^{s-1} \quad (10)$$

$$\times \left[(1 - \exp(-\beta/\mathfrak{Z}))^\alpha \right]^{n-D-s} \times \left[(1 - \exp(-\beta/T^*))^\alpha \right]^{-(n-D)}; \quad \mathfrak{Z} > T^*$$

Using Eqs. (9) and (10), the predictive log-likelihood function, dropping the constant term, can be written as Eq. (11).

$$l(\mathfrak{Z}, \alpha, \beta) = (D+1) \ln \alpha + (D+1) \ln \beta + (\alpha-1) \left[\ln(1 - \exp(-\beta/\mathfrak{Z})) + \sum_{i=1}^D \ln(1 - \exp(-\beta/t_{i:n})) \right] - 2 \left[\ln \mathfrak{Z} + \sum_{i=1}^D \ln t_{i:n} \right] - \beta \left[\mathfrak{Z}^{-1} + \sum_{i=1}^D t_{i:n}^{-1} \right] + (n-D+s) \ln \left[(1 - \exp(-\beta/\mathfrak{Z}))^\alpha \right] + (s-1) \ln \left[(1 - \exp(-\beta/T^*))^\alpha - (1 - \exp(-\beta/\mathfrak{Z}))^\alpha \right] \quad (11)$$

So, the prediction of \mathfrak{Z} is readily obtained by solving the equations $\partial l(\mathfrak{Z}, \alpha, \beta) / \partial \mathfrak{Z} = 0$, $\partial l(\mathfrak{Z}, \alpha, \beta) / \partial \alpha = 0$, and $\partial l(\mathfrak{Z}, \alpha, \beta) / \partial \beta = 0$. These equations can be evaluated numerically by some suitable procedures.

3.1.2. Bayesian approach

In this subsection, we compute the prediction of $\tau = T_{s+D:n}$ based on $T_{1:n}, \dots, T_{D:n}$ using a Bayesian approach (PBP). For this purpose, we assumed that α and β have independent gamma prior distributions with the following probability density functions:

$$\pi(\alpha) \propto \alpha^{a-1} e^{-b\alpha} \quad \text{and} \quad \pi(\beta) \propto \beta^{c-1} e^{-d\beta} \quad (12)$$

From Eq. (9), the joint posterior up to proportionality can be written as:

$$\pi(\alpha, \beta|T) \propto \alpha^{D+a-1} \beta^{D+c-1} e^{-b\alpha-d\beta} \left((1 - \exp(-\beta/T^*))^\alpha \right)^{n-D} \prod_{i=1}^D \frac{1}{t_i^2} \exp(-\beta/t_i) [1 - \exp(-\beta/t_i)]^{\alpha-1} \quad (13)$$

Therefore using Eqs. (10) and (11), the Bayesian predictive distribution can be written as [21,22]:

$$f^*(\mathfrak{Z}|T) = \int_0^\infty \int_0^\infty f(\mathfrak{Z}|T) \pi(\alpha, \beta|T) d\alpha d\beta \quad (14)$$

Eq. (14) cannot be evaluated analytically. Therefore, a Markov chain Monte Carlo (MCMC) sample is used to obtain the consistent estimator $f^*(\mathfrak{Z}/T)$ (see [23-27]). The Bayesian point predictors of $\mathfrak{Z} = T_{s+D:n}$ under a square ($L(\theta, \hat{\theta}) = (\theta - \hat{\theta})^2$) and Linex ($L(\theta, \hat{\theta}) = (e^{c(\hat{\theta}-\theta)} - c(\hat{\theta}-\theta) - 1); c \neq 0$) loss functions are:

$$\hat{\mathfrak{Z}}_{BL-Square} = \int_{T^*}^\infty \mathfrak{Z} f^*(\mathfrak{Z}|T) d\mathfrak{Z} \quad \text{and} \quad (15)$$

$$\hat{\mathfrak{Z}}_{BL-Linex} = \frac{-1}{c} \ln \left[\int_{T^*}^\infty e^{-c\mathfrak{Z}} f^*(\mathfrak{Z}|T) d\mathfrak{Z} \right]$$

3.2. Interval Prediction

A prediction interval is an interval which uses the results of a past sample and contains the results of a future sample from the same population with a specified probability. In this subsection, we consider the prediction intervals of $\mathfrak{Z} = T_{s+D:n}$ based on $T_{1:n}, \dots, T_{D:n}$. A 100(1- γ)% prediction interval for $\mathfrak{Z} = T_{s+D:n}$ can be written as $(L(T), U(T))$ such that $P(L(T) < \mathfrak{Z} < U(T)) = 1 - \gamma$.

3.2.1. Pivotal Quantity

We chose $\mathfrak{R} = 1 - \frac{[1 - \exp(-\beta/\mathfrak{Z})]^\alpha}{[1 - \exp(-\beta/T^*)]^\alpha}$; $\mathfrak{R} \sim \text{Beta}(s, n-D+s+1)$

as a pivotal quantity for obtaining the prediction interval for $\mathfrak{Z} = T_{s+D:n}$. So, the prediction interval for $\mathfrak{Z} = T_{s+D:n}$ is given by Eq. (16) [28]:

$$\left(\left(-\frac{1}{\beta} \ln \left(1 - \left(\lambda(T^*) (1 - B_{\gamma/2}) \right)^{1/\alpha} \right) \right)^{-1}, \left(-\frac{1}{\beta} \ln \left(1 - \left(\lambda(T^*) (1 - B_{1-\gamma/2}) \right)^{1/\alpha} \right) \right)^{-1} \right) \quad (16)$$

where, $\lambda(T^*) = [1 - \exp(-\beta / T^*)]^\alpha$ and B_γ are the percentile of $Beta(s, n-D+s+1)$.

3.2.2. Bayesian Interval

In this subsection, using the Eq. (14), we obtain the symmetric $100(1-\gamma)\%$ predictive interval ($L_{Bayes}(T)$, $U_{Bayes}(T)$) for $\mathfrak{Z} = T_{s+D:n}$ by solving the following two nonlinear equations:

$$P(T_{s+D:n} > L_{Bayes}(T)|T) = \frac{1-\gamma}{2} \quad \text{and} \quad (17)$$

$$P(T_{s+D:n} < U_{Bayes}(T)|T) = \frac{1+\gamma}{2}$$

where, $P(\mathfrak{Z} = T_{s+D:n} > q|T) = \int_q^\infty f^*(\mathfrak{Z}|T)d\mathfrak{Z}$ and we can also use the MCMC approach to sample from Eq. (14).

4. Existing experimental data

In this section, we analyze the data of the maximum spreading diameter of nanoparticles obtained in Hai-Bao *et al.* [4]. The data consists of the maximum diameter obtained on hydrophobic surfaces. Four different nanoparticle impact velocities were used to find data on two surfaces with contact angles of $\theta=110^\circ$ and $\theta=130^\circ$. We first drew the surface evaluation data plot in Fig. 4. It is observed that for fixed contact time, as the impact velocity increases, the maximum spreading diameter of nanoparticle increases. For clarification, we present the box-plot of this data in Fig. 5. This plot shows the descriptive statistics of the proposed data. The solid line in the box represents median value and the box represents the 25-75% percentiles. Also, the range bar represents 5 and 95% percentiles. Some positive asymmetry exists as $Median-Upper\ Quartile > Lower\ Quartile-Median$. Also, we see that there are no outliers in the data set.

After obtaining the previous data, we then compared the proposed model (generalized inverted exponential model) with the three following models:

- Generalized Inverted Exponential Model (Model 1),
- Inverse Weibull Model (Model 2),
- Inverse Gamma Model (Model 3),
- Inverse Kumaraswamy Model (Model 4).

The maximum likelihood approach (MLE) is considered to evaluate the model's associated parameters. Table 1 represents the MLEs of the model parameters and the following criteria;

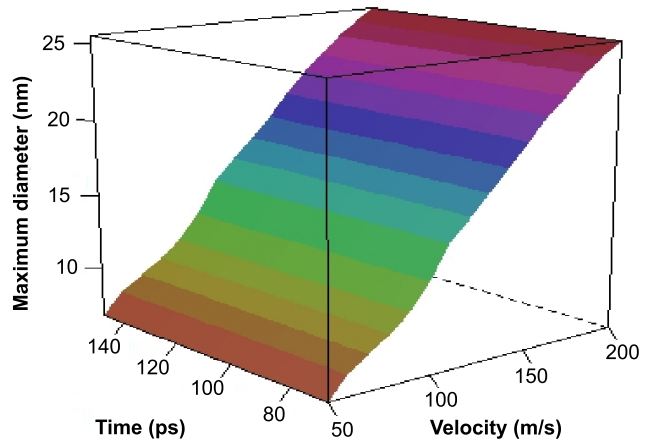


Fig. 4. The surface evaluation data plot.

- Akaike information criterion (AIC):
 $AIC = 2(\text{Number of model's parameters}) - 2\log(\text{Likelihood Function of the model})$
 - Bayesian information criterion (BIC):
 $BIC = (\text{Number of model's parameters}) \times \log(\text{Sample size}) - 2\log(\text{Likelihood function of the model})$
 - Log-likelihood (-Log L) values:
 $-\text{Log } L = -\log(\text{Likelihood function of the model})$
- The results indicate that the generalized inverted exponential model (model 1) has the lowest AIC, BIC, and values, and so was chosen as the adequate and best model. We also employed two further tests to check whether the proposed model (model 1) is a valid model for maximum spreading diameter of nanodroplets data. We considered the following tests:
- Kolmogrov-Smirnov test (Ψ_{KS}):
 $\Psi_{KS} = \text{Sup}|\text{Empirical distribution function} - \text{Distribution function}|.$
 - Anderson-Darling test (Ψ_{AD}):

$$\Psi_{AD} = n \int_{-\infty}^{\infty} \frac{(\text{Empirical Distribution Function} - \text{Distribution Function})^2}{(\text{Distribution Function}) \times (\text{Survival Function})}$$

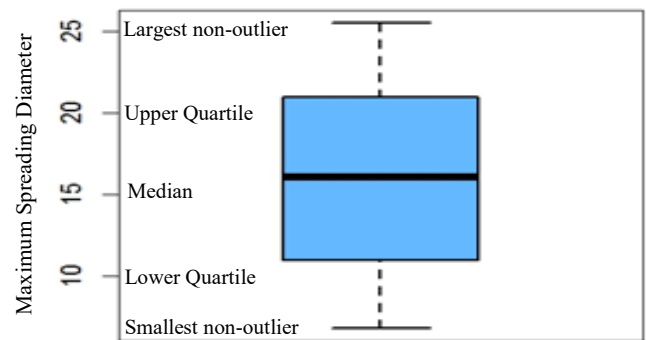


Fig. 5. Box-plot of maximum diameter of nano droplets data

Table 1. MLEs, AICs, BICs, and -logL for the different models.

Models	MLEs	AIC	BIC	-LogL
Model 1	$\alpha=15.4947$ $\beta=47.1558$	198.1123	200.9803	97.05615
Model 2	$\alpha=2.74542$ $\beta=12.3989$	203.4704	206.3384	99.73521
Model 3	$\alpha=7.28943$ $\beta=101.8324$	199.6479	202.5159	97.82397
Model 4	$\alpha=2279.725$ $\beta=2.97415$	202.9685	205.8365	99.48426

The results presented in Table 2 show that the proposed model has the smallest Ψ_{KS} and Ψ_{AD} values. So, we concluded that this model is good for analysis of the data.

Table 2. The values of Ψ_{KS} and Ψ_{AD} for the different models.

Tests	Model 1	Model 2	Model 3	Model 4
Ψ_{KS}	0.1141092	0.1291207	0.1225878	0.1275466
Ψ_{AD}	0.6504538	0.7781973	0.6775507	0.7540557

For more comparison, the empirical distribution function and the cumulative distribution function (CDF) plot as well as the probability-probability (P-P) plot and the quantile-quantile (Q-Q) plot are also given to show the appropriateness of model 1 for the considered data set; see Figs. 6-8, respectively. Based on Fig. 6, we observe that the fitted survival function of Model 1 is identical and fits the data well. Furthermore, Figs. 7 and 8, show the data do not deviate dramatically from the line.

Now, we consider the prediction problem of the censored data using the observed data. For comparison purposes, we considered the three different cases for censored data.

- Case 1: $n = 31, T_1 = 23, T_2 = 24, X_r = 17.377$
- Case 2: $n = 31, T_1 = 23, T_2 = 24, X_r = 23.450$
- Case 3: $n = 31, T_1 = 23, T_2 = 24, X_r = 25.535$

In cases 1, 2 and 3, we observed 27, 28 and 29 data. So, we predict the as $\mathfrak{S} = T_{s+D:n}$ ($s = 1, 2, \dots, n-D$):

- Case 1: $\mathfrak{S} = T_{s+27:31}$ ($s = 1, 2, 3, 4$)
- Case 2: $\mathfrak{S} = T_{s+28:31}$ ($s = 1, 2, 3$)
- Case 3: $\mathfrak{S} = T_{s+29:31}$ ($s = 1, 2$)

The different point and interval predictors of

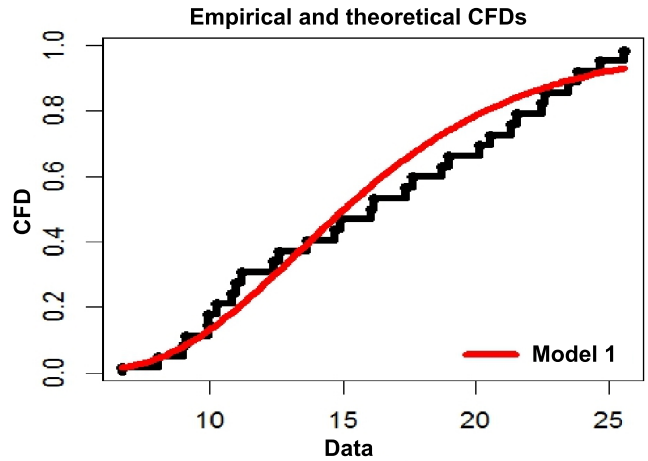


Fig. 6. Empirical and cumulative distribution function based on the maximum diameter data.

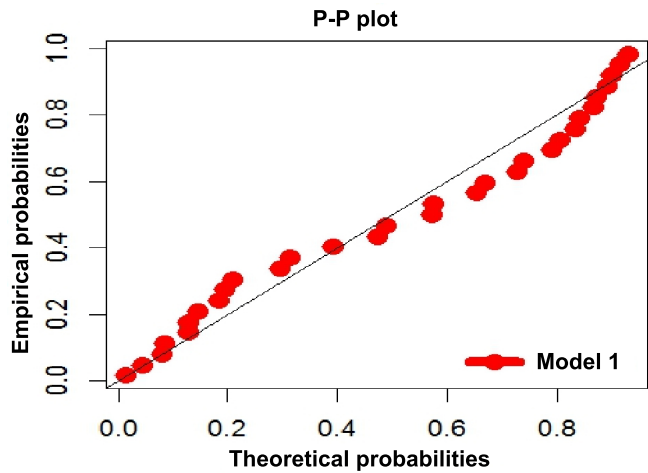


Fig. 7. The P-P plot based on the maximum diameter data.

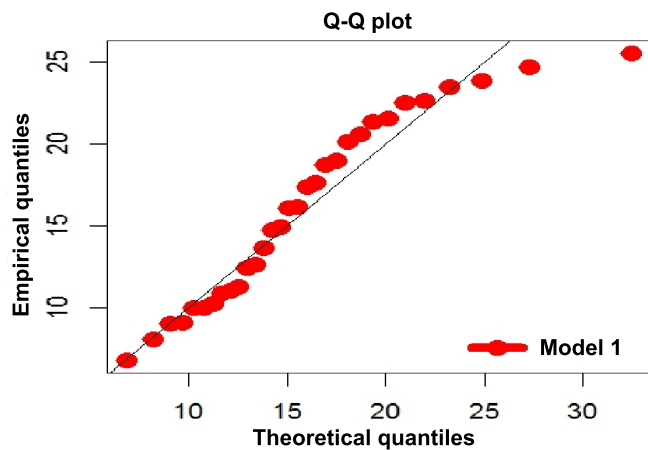


Fig. 8. The Q-Q plot based on the maximum diameter data.

$\mathfrak{S} = T_{s+D:n}$ ($s = 1, 2, \dots, n-D$) are computed using the different methods discussed in this section. The results are displayed in Tables 3 and 4, respectively.

From Table 3, it is observed that the different point predictors are quite close to the true values. Also, it is

clear that the different prediction intervals contain the true values, and this verifies the applicability of the prediction techniques for real data.

5. Conclusion

In this paper, we considered the estimation of the unavailable or censored maximum spreading diameter of nanoparticle data for the impact of a nanodroplet on hydrophobic surfaces. Since it is not possible to observe complete data in many experiments of nano coating processes, prediction of a future sample, based on the currently available sample, is very important in the analysis of experimental data. In the present work, we have considered a potential model to estimate the maximum spreading diameter of nanoparticle data. A detailed description of the proposed model, its parameter estimation, and model selection techniques have been provided. Based on the proposed model, we provided the point and interval prediction of the censored maximum spreading diameter of nanoparticle data. The obtained results indicate that the proposed point methods work well and the interval methods include the corresponding real values.

Table 3. Different point prediction values.

Cases	s	True Values	PLP	PBP
Case 1	1	23.4500	23.3733	23.5421
	2	23.8280	23.8629	23.9157
	3	24.6810	24.7643	24.8893
	4	25.5350	25.6853	25.7732
Case 2	1	23.8280	23.8474	23.8745
	2	24.6810	24.7735	24.8233
	3	25.5350	25.6596	25.7198
Case 3	1	24.6810	24.7121	24.8020
	2	25.5350	25.5936	25.6792

Table 4. Different interval prediction values.

Cases	s	True Values	PLP	PBP
Case 1	1	23.4500	(22.92,25.96)	(22.59,26.09)
	2	23.8280	(23.01,26.58)	(22.87,26.65)
	3	24.6810	(23.33,26.89)	(23.16,26.97)
	4	25.5350	(23.61,27.06)	(23.25,27.19)
Case 2	1	23.8280	(22.47,26.97)	(22.21,27.11)
	2	24.6810	(23.33,27.57)	(23.16,27.73)
	3	25.5350	(23.62,27.81)	(23.27,27.92)
Case 3	1	24.6810	(24.03,28.38)	(23.93,28.52)
	2	25.5350	(24.21,28.86)	(24.05,29.07)

Nomenclature

AIC	Akaike information criterion
BIC	Bayesian information criterion
U	Random variable which is uniformly
D	Number of observed data
T	Positive random variable
t	Value of the positive random variable
$f_r(t)$	Probability density function
$F_r(t)$	Cumulative distribution function
α	Unknown shape parameter of the model
β	Unknown scale parameter of the model
$r_T(t)$	Hazard function
$h_T(T)$	Reliability function
$Q(u)$	Quantile function
$T_{1:n} < \dots < T_{n:n}$	Random sample of size n from generalized inverted exponential model
$T_{1:n} < \dots < T_{D:n}$	Observed sample
T^*	Termination time of the experiment
T_{S+DN}	s^{th} Future order statistic where $s = 1, 2, \dots, n-D$
$\pi(0)$	Gamma prior distribution
$\pi(\alpha, \beta T)$	Joint posterior distribution
$f^*(T_{S+D:n} T)$	Bayesian predictive distribution
$L(\theta, \hat{\theta})$	Loss function
$\mathfrak{S}_{BL-Square}$	Bayesian point predictor under a square error loss function
$\mathfrak{S}_{BL-Linear}$	Bayesian point predictor under a Linex error loss function
\mathfrak{R}	Pivotal quantity
$L_{Bayes}(T)$	Lower predictive interval
$U_{Bayes}(T)$	Upper predictive interval
γ	Upper percentile of the standard normal distribution
Ψ_{KS}	Kolmogrov-Smirnov test
Ψ_{AD}	Anderson-Darling test

References

[1] S.C. Maroo, J.N. Chung, Nanodroplet impact on a homogenous surface using molecular dynamics, ASME 2008 3rd Energy Nanotechnology International Conference, ENIC2008-53036 (2008) 113-121.

[2] N. Sedighi, S. Murad, S.K. Aggarwal, Molecular dynamics simulations of nanodroplet spreading on solid surfaces, effect of droplet size, Fluid Dyn. Res. 42 (2010) 035501.

- [3] S. Asadi, Simulation of nanodroplet impact on a solid surface, *Int. J. Nano Dimens.* 3 (2012) 19-26.
- [4] H. Hai-Bao, C. Li-Bin, B. Lu-Yao, H. Su-He, Molecular dynamics simulations of the nanodroplet impact process on hydrophobic surfaces, *Chinese Phys. B*, 23 (2014) 074702.
- [5] X.-H. Li, X.-X. Zhang, M. Chen, Estimation of viscous dissipation in nanodroplet impact and spreading, *Phys. Fluids*, 27 (2015) 052007.
- [6] K. Kobayashi, K. Konno, H. Yaguchi, H. Fujii, T. Sanada, M. Watanabe, Early stage of nanodroplet impact on solid wall, *Phys. Fluids*, 28 (2016) 032002.
- [7] S. Asadi, Simulation of nanodroplet impact on an oblique surface in nanocoating processes by molecular dynamics, *Iran. J. Surface Sci. Eng.* 13 (2017) 41-50.
- [8] H. Panahi, S. Asadi, Statistical modeling for oblique collision of nano- and microdroplets in plasma spray processes, *Int. J. Nanosci. Nanotech.* 14 (2018) 71-83.
- [9] H.M. Khan, S.B. Provošt, A. Singh, Predictive inference from a two-parameter Rayleigh life model given a doubly censored sample, *Commu. Stat.-Theor. M.* 39 (2010) 1237-1246.
- [10] E.A. Ahmed, Estimation and prediction for the generalized inverted exponential distribution based on progressively first-failure-censored data with application, *J. Appl. Stat.* 44 (2017) 1576-1608.
- [11] H. Panahi, S. Asadi, Modeling of splat particle splashing data during thermal spraying with the Burr distribution, *J. Part. Sci. Technol.* 3 (2017) 41-50.
- [12] J.Y. Chiang, S. Wang, T.-R. Tsai, T. Li, Model selection approaches for predicting future order statistics from Type II censored data, *Math. Probl. Eng.* 4 (2018) 3465909.
- [13] I. Basak, N. Balakrishnan, A note on the prediction of censored exponential lifetimes in a simple step-stress model with type-II censoring, *Calcutta Stat. Assoc.* 70 (2018) 57-73.
- [14] A.M. Abouammoh, M.A. Alshingiti, Reliability estimation of generalized inverted exponential distribution, *J. Stat. Comput. Sim.* 79 (2009) 1301-1315.
- [15] S. Nadarajah, S. Kotz, The exponentiated type distributions, *Acta Appl. Math.* 92 (2006) 97-111.
- [16] S. Kotz, S. Nadarajah, *Extreme value distributions: Theory and applications*, Imperial College Press, London (2000).
- [17] H. Panahi, Estimation methods for the generalized inverted exponential distribution under Type II progressively hybrid censoring with application to spreading of microdrops data, *Commun. Math. Stat.* 5 (2017) 159-174.
- [18] E.A., Ahmed, Estimation and prediction for the generalized inverted exponential distribution based on progressively first-failure censored data with application, *J. Appl. Stat.* 44 (2017) 1576-1608.
- [19] B. Chandrasekar, A. Childs, N. Balakrishnan, Exact likelihood inference for the exponential distribution under generalized Type-I and Type-II hybrid censoring, *Nav. Res. Log.* 51 (2004) 994-1004.
- [20] A. Shafay, Bayesian estimation and prediction based on generalized Type-II hybrid censored sample, *J. Stat. Comput. Sim.* 86 (2016) 1970-1988.
- [21] R. Valiollahi, A. Asgharzadehb, D. Kundu, Prediction of future failures for generalized exponential distribution under Type-I or Type-II hybrid censoring, *Braz. J. Probab. Stat.* 31 (2015) 1-21.
- [22] A.J. Fernández, On maximum likelihood prediction based on Type II doubly censored exponential data, *Metrika*, 3 (2000) 211-220.
- [23] D. Kundu, H. Howlader, Bayesian inference and prediction of the inverse Weibull distribution for Type-II censored data, *Comput. Stat. Data Anal.* 54 (2010) 1547-1558.
- [24] S.O. Bleed, Gibbs sampling and Bayesian estimators for time censoring constant stress reliability/life prediction, *J. Hum. Appl. Sci.* 28 (2016) 166-182.
- [25] E. Saraiva, A. Suzuki, L. Milan, Bayesian computational methods for sampling from the posterior distribution of a bivariate survival model, based on AMH copula in the presence of right-censored data, *Entropy*, 20 (2018) 35-42.
- [26] S. Sel, M. Jung, Y. Chung, Bayesian and maximum likelihood estimations from parameters of McDonald Extended Weibull model based on progressive Type-II censoring, *J. Stat. Theor. Pract.* 12 (2018) 231-254.
- [27] H. Panahi, Inference for exponentiated Pareto distribution based on progressive first-failure censored data with application to cumin essential oil data, *J. Stat. Manag. Sys.* 21 (2018) 1433-1457.
- [28] H.L. Lu, Prediction intervals of an ordered observation from one-parameter exponential distribution based on multiple Type II censored samples, *J. Chin. Inst. Ind. Eng.* 21 (2004) 494-503.